

# Label-Efficient Online Continual Object Detection in Streaming Video

Jay Zhangjie Wu<sup>1</sup>, David Junhao Zhang<sup>1</sup>, Wynne Hsu<sup>2</sup>, Mengmi Zhang<sup>3</sup>, Mike Zheng Shou<sup>1\*</sup>

<sup>1</sup> Show Lab, National University of Singapore

<sup>2</sup> School of Computing, National University of Singapore

<sup>3</sup> CFAR and I2R, Agency for Science, Technology and Research

## Abstract

To thrive in evolving environments, humans are capable of continual acquisition and transfer of new knowledge, from a continuous video stream, with minimal supervisions, while retaining previously learnt experiences. In contrast to human learning, most standard continual learning benchmarks focus on learning from static iid images in fully supervised settings. Here, we examine a more realistic and challenging problem—Label-Efficient Online Continual Object Detection (LEOCOD) in video streams. By addressing this problem, it would greatly benefit many real-world applications with reduced data annotation costs and model retraining time. To tackle this problem, we seek inspirations from complementary learning systems (CLS) in human brains and propose a computational model, dubbed as Efficient-CLS. Functionally correlated with the hippocampus and the neocortex in CLS, Efficient-CLS posits a memory encoding mechanism involving bidirectional interaction between fast and slow learners via synaptic weight transfers and pattern replays. We test Efficient-CLS and competitive baselines in two challenging real-world video stream datasets. Like humans, Efficient-CLS learns to detect new object classes incrementally from a continuous temporal stream of non-repeating video with minimal forgetting. Remarkably, with only 25% annotated video frames, our Efficient-CLS still leads among all comparative models, which are trained with 100% annotations on all video frames. The data and source code will be publicly available at <https://github.com/showlab/Efficient-CLS>.

## 1 Introduction

Humans have the ability to continuously learn from an ever-changing environment, while retaining previously learnt experiences. In contrast to human learning, recent works in continual learning[2, 1, 8, 27, 4] show that deep neural networks (DNNs) are prone to catastrophic forgetting. Online Continual Learning (OCL) remains a challenging problem where an agent learns from a never-ending stream of data in only a single pass. Existing works in OCL [2, 1, 8, 4] primarily focus on image classification tasks. However, later works [18, 27] show that these methods underperform in more complex vision tasks, such as object detection. Moreover, these experiments in incremental image classification are conducted in an idealistic and simplified scenario when a list of object classes is learnt in a fixed order, and the learnt classes become inaccessible after being presented once. It deviates from the OCL in the real world where novel classes could co-occur with learnt classes in the same scene due to context regularities.

Here, to imitate what humans see and learn, we examine a more realistic and challenging problem of online continual object detection in real-world video streams. Although teaching machines to continuously detect objects on every video frame with full supervision is the most ideal, annotating

---

\*Corresponding Author.

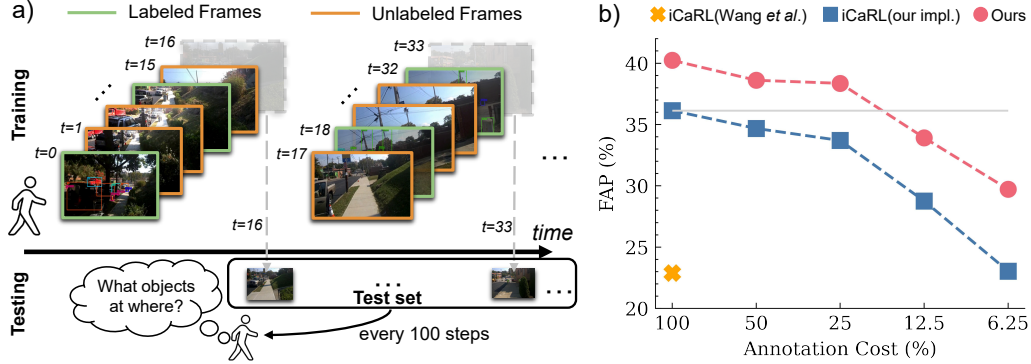


Figure 1: **Label-efficient online continual object detection in video streams.** (a) Problem introduction: As an agent continuously learns from a video stream, the ground truth labels from a certain percentage number of the video frames (green boundary) are revealed to the agent, while the majority of frames (orange boundary) are annotation-free. We define annotation cost as the proportion of the number of annotated video frames out of a mini-batch containing 16 consecutive video frames. To construct a test set, the last video frame (transparent) from every mini-batch is held out for testing, and it is not presented to the agent during training. We stamp every learning step from a mini-batch as a time step. After every 100 time steps, the agent is evaluated on all the images from the test set for object detection. (b) Our proposed model (red) outperforms the best competitive baseline (blue) by a margin of 5% over all proportions of annotation costs. Remarkably, our model, trained at 25% annotation costs, surpasses the best baseline trained at 100% annotation costs (grey line). The orange cross denotes the performance of the state-of-the-art model, which is 15% lower than ours.

bounding boxes for all objects and labeling their corresponding object classes per video frame is a very daunting task. Here, our goal is to study online continual object detection problem in video streams with minimal amount of annotations. We introduce our problem setting in Figure 1.

Our work shares similar motivations with works in semi-supervised learning. Over the past few years, several object detection approaches [17, 31, 26] in semi-supervised learning have been proposed to reduce annotation costs. However, they follow an offline training protocol where labeled and unlabeled data can be used repeatedly across hundreds of epochs. Moreover, these studies focus on object detection problem in static independent and identically distributed (iid) images and discard the temporal correlation in the real-world videos. To our best knowledge, we are the first to study label-efficient online continual object detection in video streams.

Cognitive science works [28, 16] show that humans are efficient at continuously learning from very few annotated data samples. We get inspirations from the theory of Complementary Learning System (CLS) in human brains, and propose a general framework for Label-Efficient Online Continual Object Detection, dubbed as Efficient-CLS model. In particular, CLS theory postulates that the memories are first encoded via fast synaptic changes in the hippocampus and then these changes support slow reinstatement of memories in the neocortex via accumulated experiences over time [15]. To mimic the fast and slow synaptic changes in hippocampus and neocortex, in Efficient-CLS, we introduce two feed-forward neural networks as slow and fast learners. In the fast learner, memory is encoded in its synaptic weights and these weights adapt rapidly to the current task. The synapses of the slow learner change a little on each reinstatement, and are maintained by taking the exponential moving average of the fast learner’s synapses over time. Though a few continual learning models in previous works [3, 20] also use a similar source of inspiration, they miss the effect of reciprocal connections from neocortex to hippocampus, which we intend to address. The neuroscience study [12] has identified the importance of bidirectional interaction between the two complementary systems, whereby the reactivation of neural patterns in the neocortex triggers replays in the hippocampus, which in turn drive the memory consolidation in the neocortex. Inspired by this underlying mechanism, we reactivate the weights of the slow learners to predict meaningful pseudo labels from the unlabeled video frames and use these pseudo labels to guide the training of the fast learner, closing the loop between the two complementary learning systems. Specifically, pseudo labels, predicted by the slow learner, carry integrated semantic information over time, which encourages the fast learner to capture more holistic scene representations, alleviating the catastrophic forgetting problem on sparsely annotated videos.

We benchmark our method on online continual object detection with video streams from OAK and EgoObjects datasets. We conduct comprehensive experiments to evaluate the effectiveness of our method in alleviating catastrophic forgetting and reducing annotation costs. Our model Efficient-CLS consistently outperforms the existing methods by a large margin of 5% over all annotation costs. At only 25% annotation costs, Efficient-CLS even surpasses all the comparative baseline models trained with 100% annotation costs. Our contributions of this paper are two-fold:

- We introduce a new, challenging and important problem of label-efficient online continual object detection in video streams. Solving this problem would greatly benefit real-world applications in minimizing annotation costs and reducing model retraining time.
- To tackle this problem, we propose a computational model inspired from the theory of Complementary Learning System. It beats all competitive baselines in object detection tasks by a large margin with minimal forgetting and minimal amount of annotations.

## 2 Related Work

### 2.1 Complementary Learning System (CLS)

The essence of fast and slow learning in CLS has benefited several continual learning applications in object recognition [20, 19, 23, 3, 13]. However, these methods either require the task boundaries, which are not applicable in our online problem setting, or they require to train fast and slow learning systems with replay samples from the same replay buffer, which could easily lead to overfitting problem when the replay buffer has limited capacity. To eliminate overfitting problem, Rostami *et al.* [23] and Kamra *et al.* [13] utilized generative replay models to couple sequential tasks in a latent embedding space. However, generative approaches have succeeded in artificial and simple datasets, but have failed in complex vision tasks, *e.g.* object detection. Based on the neuroscience evidence of the bidirectional interaction between the hippocampus and the neocortex [6], we leverage slow learners to exploit unlabeled video frames and generate pseudo labels for training fast learners. These pseudo label replays encourage fast learners to capture more generic representations from diverse data of replay buffers and unlabeled video frames; hence, in turn, contributing to reinstatement of memory in slow learners, resulting in a positive feedback loop.

### 2.2 Online Continual Learning (OCL)

In contrast to classical Continual Learning (CL) where data are separated by task boundaries and models are trained with multiple iterations in every task, we examine a more realistic and challenging problem where data are provided in tiny batches and models are trained on these batches only once. OCL has gained increasing interests recently in computer vision [2, 4, 24, 5, 27]. Many OCL methods rely on representative memory replays. Aljundi *et al.* [2] utilized gradients of network parameters to select replay samples of maximum diversity. Subsequent works [1, 24] proposed to use losses and scoring functions as criteria for selecting the most representative samples for replays. However, these approaches tackled image classification problem in an artificial setting, where new classes appear in a specific order. Their performance in real-world vision tasks remains unclear. Lately, Wang *et al.* [27] benchmarked OCL methods in the real-world setting with full supervisions. As the video streams arrive endlessly in a real-time manner, assigning annotations to all the video frames for training computational models is laborious and time-consuming. It becomes even more daunting in object detection tasks where class labels and bounding boxes of all objects on a video frame have to be provided. Reducing burdensome costs of labeling remains an under-explored and challenging problem in OCL. We propose a self-sustaining Efficient-CLS. Our model is capable of exploiting the unlabeled video frames by pseudo-labeling when the number of labeled frames is limited.

### 2.3 Semi-Supervised Object Detection (SSOD)

To reduce annotation costs in object detection, several methods [11, 25, 17] capitalize the teacher-student networks. In general, a teacher model predicts pseudo labels or enforces a consistency loss to guide the student networks. Recently, Liu *et al.* [17] proposed to use Exponential Moving Average (EMA) to update the teacher model. It is worth noting that these previous works on SSOD mainly consider the offline setting on static image datasets, while none of them has been extended to online video streams.

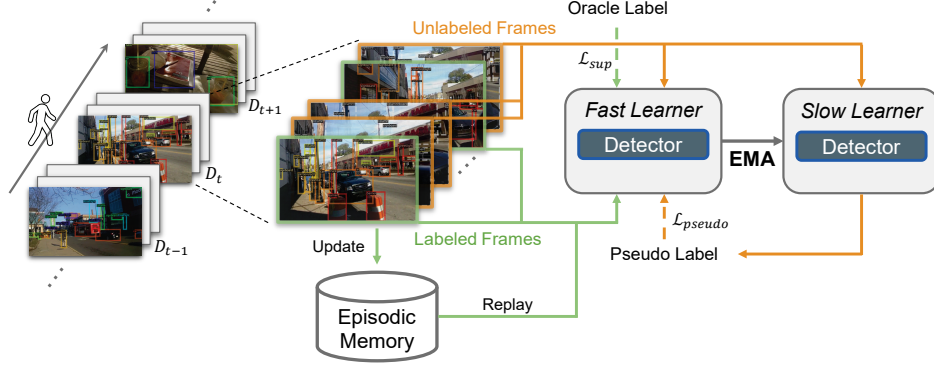


Figure 2: **The overview of our Efficient-CLS.** At each learning step, the system receives a batch of temporally continuous data  $D_t$ , including labeled (green) and unlabeled (orange) frames. The fast learner trains the labeled frames alongside a small subset of labeled exemplars retrieved from episodic memory with the supervised loss  $\mathcal{L}_{sup}$ . Meanwhile, the fast learner leverages the pseudo labels generated by the slow learner to optimize a pseudo loss  $\mathcal{L}_{pseudo}$ . To reinstate memory of the slow learner, the synaptic weights of the slow learner are updated by taking the Exponential Moving Average (EMA) of the fast learner’s weights. The fast and slow learners are complementary to each other, forming a positive feedback loop.

### 3 Efficient-CLS: Efficient Complementary Learning System

We consider the online continual object detection on a continuum of video streams  $\mathcal{D} = \{D_1, \dots, D_T\}$  where at time step  $t$ , a learning agent receives a mini-batch of continuous video frames  $D_t$  from current environment for online training (one single pass). To perform label-efficient object detection, within the batch  $D_t$ , only a subset of video frames  $D_t^s = (X_t^s, Y_t^s)$  are labeled, while the remaining video frames  $D_t^u = (X_t^u)$  are unlabeled. For each labeled data sample, its annotation contains the bounding box locations and their corresponding class labels.

Efficient-CLS consists of two feed-forward modules: (i) the fast learner is designed to quickly encode new knowledge from current data stream and then consolidate it to the slow learner; and (ii) the slow learner accumulates the acquired knowledge from fast learner over time and guides the fast learner with meaningful pseudo labels, when full supervision is not available. Following [21], we maintain an external episodic memory, as a replay buffer, to store exemplars that can be retrieved for replays alongside ongoing video stream.

#### 3.1 Learning with Labeled Frames

The fast learner and slow learner use the same standard Faster-RCNN [22] detector  $f$ . Despite the same architecture, the weights of the fast and slow learners are not shared. We use  $\theta_F$  and  $\theta_S$  to denote the network parameters for fast and slow learners respectively. As shown in Figure 2, at each training step  $t$ , we use the labeled video frames  $D_t^s = (X_t^s, Y_t^s)$  to optimize the fast learner  $\theta_F$  with the standard supervised loss  $\mathcal{L}_{sup}$  in Faster-RCNN [22]. It consists of four losses: Region Proposal Network (RPN) classification loss  $\mathcal{L}_{cls}^{rpn}$ , RPN regression loss  $\mathcal{L}_{reg}^{rpn}$ , Region of Interest (ROI) classification loss  $\mathcal{L}_{cls}^{roi}$ , and ROI regression loss  $\mathcal{L}_{reg}^{roi}$ . We define  $\mathcal{L}_{sup}$  as:

$$\mathcal{L}_{sup} = \mathcal{L}_{cls}^{rpn}(X_t^s, Y_t^s) + \mathcal{L}_{reg}^{rpn}(X_t^s, Y_t^s) + \mathcal{L}_{cls}^{roi}(X_t^s, Y_t^s) + \mathcal{L}_{reg}^{roi}(X_t^s, Y_t^s). \quad (1)$$

#### 3.2 Learning with Unlabeled Frames

We introduce a pseudo-labeling paradigm to capitalize the information from unlabeled video frames  $D_t^u = (X_t^u)$  for training. In our early exploration, we intuitively use the fast learner for pseudo-labeling as it quickly adapts the knowledge of nearby frames. However, we observe that using the pseudo labels generated by the fast learner for self-replay exhibits biases towards recently seen objects, which is less effective in preventing forgetting. This has also been verified in our ablation study (Section 5.3). In contrast, the slow learner preserves the semantic knowledge over a longer time span which generates pseudo labels with fewer biases. This encourages the fast learner to capture

more generic scene representations, hence, in turn, contributing to reinstatement of memory in the slow learner (Section 3.3), resulting in a positive feedback loop.

Given all these design considerations, the slow learner takes the unlabeled video frames  $D_t^u$  as inputs to estimate the possible objects of interest and their corresponding bounding box locations. For brevity, we refer these "pseudo bounding boxes and their corresponding class labels" as "pseudo labels" in the paper. To get rid of false positives, we apply a threshold  $\tau$  to filter out bounding boxes with predicted low confidence scores. Moreover, there also exist repetitive boxes which negatively impact the quality of pseudo-labeling. To address this issue, we use the technique of class-wise non-maximum suppression (NMS) [22] to remove the overlapped boxes and get the high-quality pseudo labels. Formally, the procedure of pseudo label generation is summarized below:

$$Y_t^u = NMS([f(X_t^u; \theta_S)]_{>\tau}), \quad (2)$$

where  $[\cdot]_{>\tau}$  denotes the bounding box selection with confidence score larger than  $\tau$ .

Given that the video streams are captured from the egocentric perspective in the real world, head and body motions may lead to undesired motion blur effects on some video frames. To enforce our model to learn invariant object representations from these video frames, same as the previous work [32], we apply data augmentation techniques on the pseudo-labeled frames, including 2D image crops, rotations, and flipping. Note that different from image classification, the predicted bounding box locations also need to be updated accordingly after image augmentations. We denote these pseudo-labeled video frames and their re-adjusted pseudo labels after data augmentations as  $(\tilde{X}_t^u, \tilde{Y}_t^u)$ . We can then use these pseudo pairs  $(\tilde{X}_t^u, \tilde{Y}_t^u)$  to train the fast learner by optimizing the pseudo loss  $\mathcal{L}_{pseudo} := \mathcal{L}_{cls}^{roi}(\tilde{X}_t^u, \tilde{Y}_t^u) + \mathcal{L}_{reg}^{roi}(\tilde{X}_t^u, \tilde{Y}_t^u)$ . Note that we only apply pseudo losses at the ROI module, as we empirically verified that the RPN module has no effects on pseudo training (see Section A.2.4).

Overall, our Efficient-CLS is jointly trained with the following losses:  $\mathcal{L}_{total} = \mathcal{L}_{sup} + \lambda_{pseudo}\mathcal{L}_{pseudo}$ , where  $\lambda_{pseudo}$  is the weight of  $\mathcal{L}_{pseudo}$ .

### 3.3 Synapses Consolidation via Exponential Moving Average

To alleviate forgetting of obtained knowledge, we apply EMA to gradually update the slow learner with the fast learner's synaptic weights. The evolving synaptic changes in the slow learner are functionally correlated with the memory consolidation mechanism in the hippocampus and the neocortex [3]. Formally, we define EMA process as:

$$\theta_S = \alpha\theta_S + (1 - \alpha)\theta_F, \quad (3)$$

where the  $\alpha \in [0, 1]$  is EMA rate. According to the stability-plasticity dilemma, a smaller  $\alpha$  means faster adaption but less memorization. Empirically, we set  $\alpha = 0.99$ , which leads to best performance (see Section A.2.2 for detailed analysis on choices of  $\alpha$ ).

## 4 Experimental details

### 4.1 Datasets

We consider two challenging datasets, *i.e.*, OAK [27] and EgoObjects [9] for online continual object detection on video streams.

**OAK dataset** [27] is a large egocentric video stream dataset spanning nine months of a graduate student's life, consisting of 7.6 million frames of 460 video clips with a total length of 70.2 hours. The dataset contains 103 object categories. We follow [27] in the ordering of training and testing data splits. One frame every 16 consecutive video frames lasting for 30 seconds is held out to construct a test set and the remaining frames are used for training.

**EgoObjects**<sup>2</sup> is one of the largest object-centric datasets focusing on object detection task. It includes 40,000 videos (around 110 hours), covering 600 object categories. We take a subset of EgoObjects to benchmark LEOCOD (see Section A.1.3 for details). For consistency, we use the same ordering above as OAK dataset to construct the train and test data splits.

<sup>2</sup><https://sites.google.com/view/clvision2022/challenge>



## 4.2 Evaluation

**Protocol.** First, we define the annotation cost as the proportion of number of labeled frames versus the total 16 frames within a mini-batch  $D_t$ . For example, if 2 out of 16 consecutive frames within  $D_t$  get labeled, the annotation cost is  $2/16 = 12.5\%$ . The frames to be labeled are randomly selected within each mini-batch  $D_t$ . Considering that different choices of labeled frames might influence the computational model performance, for fair comparisons between models, we fix the choice of randomly selected labeled frames and use the same labeled and unlabeled frames for training all models.

Based on the various annotation costs, we introduce two training protocols: fully supervised protocol (100% annotation cost) and sparse annotation protocol (where the annotation cost is less than 100%). In Sparse Annotation protocol, we further split the training experiments based on 50%/25%/12.5%/6.25% annotation costs.

We use the same test set for evaluating computational models. As shown in Figure 1, we always add the last video frame out of every 16 video frames within a mini-batch  $D_t$  to our test set. Once the test set is constructed for each dataset, it is fixed. All the frames in the test set are repetitively used for evaluating computational models at every 100 learning steps. It is possible that some test frames might contain unseen object classes, where the model has not yet learnt to detect in the current learning step. In this case, we follow the same evaluation paradigm from the previous work [27]. As the model continuously learns from the ongoing video streams, the model gets to learn to detect more object classes. In the end of the video stream, the model should be able to detect all object classes present in the test set.

**Metrics.** We evaluate these baselines on OAK and EgoObjects datasets with three standard metrics: continual average precision (CAP), final average precision (FAP) and Forgetfulness (F) [27]. CAP shows the average performance of a continual learning algorithm over the time span of the entire video stream, while FAP denotes the final performance of a model after seeing the entire video stream. F estimates the forgetfulness of the model due to the sequential training. It takes into account the time interval between the first presence of an object category and its subsequent presence. See Appendix (Section A.1.2) for their detailed definitions.

## 4.3 Baselines

We compare our model against the following baselines: **Incremental** is a naive baseline trained sequentially over the entire video stream without any measures to avoid catastrophic forgetting; **EWC** [14] is a weight-regularization method which prevents forgetting by penalizing the changes of important parameters in previous tasks; **iCaRL** [21] is a replay method where old video frames are stored in a replay buffer and get replayed when a model learns to detect objects on new video frames; **Offline Training** is an upper bound. It trains the entire data stream over multiple epochs.

The iCaRL model implemented by Wang *et al.* [27] stands as the state-of-the-art method in online continual object detection. We reproduce their results using the released code<sup>3</sup>. When calculating RPN and ROI losses for replay samples, their iCaRL model neglects the losses of background proposals and penalizes the foreground losses according to the proportion of the current samples and replay samples. We empirically find that this trick hinders the model from effective video frame replay, thus resulting in severe forgetting. Therefore, we re-implement the iCaRL by discarding the re-weighting trick used in [27] and reverting back to the standard RPN and ROI losses. To distinguish these two different implementations, we name the Wang *et al.*'s version as **iCaRL(Wang *et al.*)** and ours as **iCaRL(our impl.)**.

## 4.4 Implementation Details

For fair comparisons, same as [27], we use pre-trained Faster-RCNN [22] with ResNet-50 backbone [10] on PASCAL VOC [7] for all the continual learning algorithms. Our replay buffer stores total 5 samples per class (around 500 frames for OAK, and 1400 for EgoObjects). This buffer size is comparable with the buffer size in **iCaRL(Wang *et al.*)** [27] and **iCaRL(our impl.)**. We also fix the number of replay samples to 16 frames per time step, which requires less training time compared

<sup>3</sup><https://github.com/oakdata/benchmark>

Table 1: **Performance of Efficient-CLS and other state-of-the-art methods on OAK and EgoObjects.** iCaRL(Wang *et al.*) denotes the model presented in [27], and iCaRL(our impl.) is the same method by our implementation. The best results are **bold-faced**. \*The results on OAK are lower than the ones presented in [27] due to different training settings, where [27] trains the data of each step by 10 epochs but in our strictly online setting we only see each step once.

	Annotation Cost	OAK			EgoObjects		
		FAP ( $\uparrow$ )	CAP ( $\uparrow$ )	F ( $\downarrow$ )	FAP ( $\uparrow$ )	CAP ( $\uparrow$ )	F ( $\downarrow$ )
Incremental*	100%	8.38	7.72	0.03	10.21	3.55	1.48
EWC*	100%	7.73	7.02	-0.12	5.15	1.60	0.57
iCaRL(Wang <i>et al.</i> )	100%	22.89	16.60	-2.95	37.61	21.71	2.79
iCaRL(our impl.)	100%	36.14	26.26	-4.89	60.80	36.41	-0.60
Ours	12.5%	33.92	23.04	-7.71	53.33	32.88	-2.92
	25%	38.36	26.64	<b>-8.20</b>	61.26	39.58	-3.48
	100%	<b>40.24</b>	<b>28.18</b>	-8.10	<b>67.05</b>	<b>40.36</b>	<b>-3.67</b>
Offline Training	100%	48.28	35.23	-	86.18	59.81	-

with [27]. We use confidence threshold  $\tau = 0.7$  to generate pseudo-labels and apply  $\alpha = 0.99$  as the EMA rate for all our experiments. For our Efficient-CLS, we use the output of the slow learner at the inference stage, as it excels at avoiding catastrophic forgetting (see Section 5.3). More training and implementation details can be found in Appendix (Section A.1.1).

## 5 Results

### 5.1 Performance in Fully Supervised Protocol

As the previous work [27] focuses on online continual object detection in video streams, we first evaluated model performance in fully supervised setting, where all video frames are paired with ground truth labels. We reported the results in the standard metrics (CAP, FAP, and F, Section 4.2) in Table 1. Our proposed method, Efficient-CLS, surpasses all the existing baselines.

An ideal video stream learning method should avoid catastrophic forgetting, while adapting to the new tasks. A trivial algorithm that only adapts to the current task without any measures to prevent catastrophic forgetting leads to the lowest FAP and CAP scores, and largest Forgetting (F) values. Indeed, **Incremental** is a lower bound among all computational models. Previous works have shown weight-regularization methods are less effective than replay methods in many continual learning tasks [30, 29], we included the weight-regularization method **EWC** for comparison. We observed that **EWC** is inferior to other competitive baselines in stream learning. Its performance is not significantly different from **Incremental** on OAK and even worse than **Incremental** on EgoObjects. It is possible that **EWC** has to utilize task boundaries to compute the weight importance, which is not applicable in video stream learning. During our implementation, we also noted that the running time of **EWC** is significantly longer than our method. One reason is that calculating Fisher Information Matrix to select the important weights in **EWC** is computationally expensive.

**iCaRL(Wang *et al.*)** outperforms **EWC** by 15.16% in FAP, 9.58% in CAP and 2.83% in F on OAK dataset. A significant performance boost is also consistently observed in EgoObjects in terms of FAP and CAP. This demonstrates that a naive image replay strategy can still play an important role in stream learning. We introduced several variations to the original design of **iCaRL(Wang *et al.*)** (see Section 4.3). Compared with **iCaRL(Wang *et al.*)**, we observed a performance boost of 13.25% in FAP, 9.66% in CAP, and 1.94% in F for **iCaRL(our impl.)** on OAK dataset. Since semantic contextual information is more important in indoor environments on EgoObjects compared to the outdoor environments in OAK dataset, we noticed that the improvement of **iCaRL(our impl.)** is even greater on EgoObjects dataset with an increase of 23.19% in FAP, 14.70% in CAP, and, 3.39% in F.

Inheriting from the benefit of image naive replays, our Efficient-CLS replays the images stored in the episodic memory buffer. In addition, we introduced a strategy of synaptic weight transfer from fast to slow learner. Our performance in fully supervised setting beats **iCaRL(our impl.)** by 4.10% and 1.92% in terms of FAP and CAP, respectively, and favorably reduces the Forgetfulness (F) by 3.21% on OAK dataset. Our model also consistently leads among all comparative methods in all

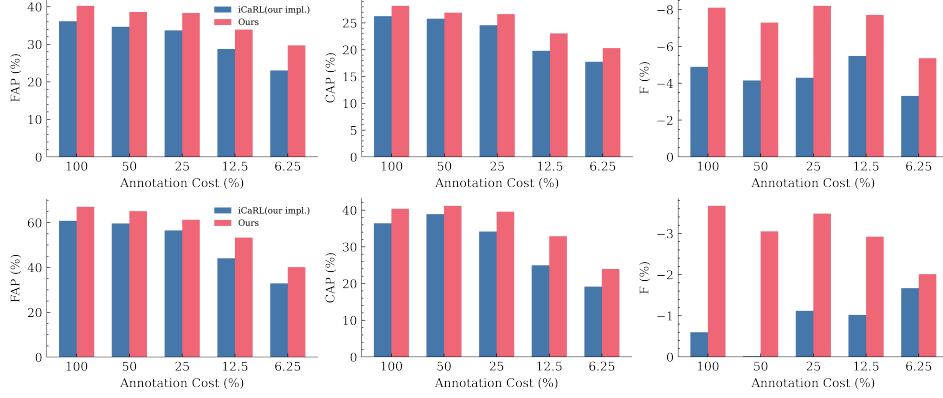


Figure 3: Evaluation of online continual object detection in video streams with three metrics (FAP, CAP and F, Section 4.2) on OAK dataset (first row) and EgoObjects dataset (second row). The higher the bars are, the better. The x-axis denotes the percentage of video frames that are labeled in the video stream. It ranges from 6.25% to 100% (full supervision). The y-axis indicates the performance using different evaluation metrics. Our method (red) consistently beats the SOTA (iCaRL(our impl.), blue) in all evaluation metrics.

evaluation metrics on EgoObjects dataset. It is worth noting that **Offline Training** provides the upper bound performance when the model is trained with the entire video streams multiple times. Despite a marginal performance sacrifice of 8.04% in FAP and CAP compared with **Offline Training**, our method significantly reduces the retraining time by 40 times, and the storage sizes by 50 times.

## 5.2 Performance in Sparse Annotation Protocol

The sparse annotation protocol is more challenging than the previous fully supervised protocol as shown by the performance differences when number of annotated video frames decreases (compare the performance of each colored bar along the x-axis within each subplot in Figure 3). We compared Efficient-CLS with the best previous method **iCaRL(our impl.)** and reported the performance in Figure 3. In both OAK and EgoObjects datasets, Efficient-CLS consistently beats the SOTA approaches in all three evaluation metrics regardless of various degrees of annotation costs. Thanks to the useful information from pseudo labels predicted by the slow learner in our Efficient-CLS, our method is more robust to various annotation costs, compared with **iCaRL(our impl.)** (compare the rate of change of blue bars vs. red bars over different degrees of annotation costs). Most remarkably, Efficient-CLS with 25% annotation costs has already outperformed **iCaRL(our impl.)** with 100% annotation costs (compare the red bar at 25% with the blue bar at 100% within each subplot).

## 5.3 Ablation Study

We assessed the importance of design choices by evaluating ablated versions of our Efficient-CLS model in fully supervised learning protocol (Table 2) and sparse annotation protocol (Table 3). The complementary learning system design in Efficient-CLS is the key for rapidly adapting to learn new tasks, meanwhile, retaining previously learnt knowledge. It constitutes of two memory reinstatement mechanisms: one is synaptic weight transfer from fast to slow learner via exponential moving average (EMA); and the other is pseudo-labeling and replays from slow learner to fast learner. Here we ablated individual mechanism and studied their effect on OAK dataset.

**Effect of Exponential Moving Average (EMA).** We removed EMA by setting  $\alpha$  to 1 in Equation 3, where the model weights of the fast learner and slow learner are now shared throughout the learning process. From Table 2 in the fully supervised protocol, we observed that removing EMA leads to a performance drop of 4.10% in FAP, 1.92% in CAP and 3.21% in F on OAK dataset (compare Row 2 vs. Row 1). This shows that the slow learner can effectively consolidate the knowledge from the fast learner, and constructively alleviate catastrophic forgetting by synapses consolidation over time. Given the fact that the slow learner is better at preventing forgetting than the fast learner, we used the output from the slow learner at the inference stage. Similar observations were made on Table 3 in



Table 2: **Effectiveness of Exponential Moving Average (EMA) on OAK dataset in fully supervised protocol.** The best results are **bold-faced**.

EMA	FAP ( $\uparrow$ )	CAP ( $\uparrow$ )	F ( $\downarrow$ )
$\times$	36.14	26.26	-4.89
$\checkmark$	<b>40.24</b>	<b>28.18</b>	<b>-8.10</b>

Table 3: **Effectiveness of Exponential Moving Average (EMA) and Pseudo-labeling on OAK dataset at annotation cost 12.5%.** The best results are **bold-faced**.

EMA	Pseudo-labeling	FAP ( $\uparrow$ )	CAP ( $\uparrow$ )	F ( $\downarrow$ )
$\times$	$\times$	28.76	19.80	-5.48
$\checkmark$	$\times$	31.72	21.16	-7.24
$\times$	$\checkmark$	31.60	22.44	-4.83
$\checkmark$	$\checkmark$	<b>33.92</b>	<b>23.04</b>	<b>-7.71</b>

the sparse annotation protocol (compare Row 4 vs. Row 3). It is worth noting that the performance difference between our full model (Row 4) and **Ablated EMA** (Row 3) is slightly larger in fully supervised protocol than the sparse annotation protocol (compare Table 2 vs. Table 3). One reason is that compared with sparse annotation protocol, the fast learner achieves better performance in fully supervised training; hence, the effect of removing EMA becomes stronger in the fully supervised setting, again highlighting the importance of EMA.

To further explore the role of EMA, we varied  $\alpha$  from 0.5 and 0.999 and reported their performance in Section A.2.2. We observed that the choice of  $\alpha$  is relatively insensitive to the performance. For example, Efficient-CLS with  $\alpha = 0.9$  leads to an performance increase of less than 1% in FAP and CAP and 1.12% in F, compared with the case of  $\alpha = 0.5$ . However, we did observe a huge performance drop when  $\alpha$  is very close to 100%, where there is almost no synaptic weight transfer between slow and fast learner.

**Effect of the Pseudo-labeling.** We ablated our Efficient-CLS by removing the pseudo-labeling and replays of the slow learner at 12.5% annotation costs (**Ablated Pseudo**, Row 2) and reported the results in Table 3. **Ablated Pseudo** leads to a performance drop of 2% in FAP and CAP and 0.5 in F, compared with our full Efficient-CLS (Row 4). It implies that the slow learner captures useful semantic information from unlabeled video frames and these predicted pseudo labels are helpful in training the fast learner.

To investigate whether pseudo labels predicted by the fast learner could help stream learning, we conducted another ablation experiment where we removed both EMA and pseudo-labeling mechanisms in Efficient-CLS, dubbed as **Naive Ablated** (Row 1, Table 3). Compared with **Ablated EMA** (Row 3), we observed a performance drop from 31.60% to 28.76% in FAP and 22.44% to 19.80% in CAP. It indicates that pseudo labels predicted by the fast learner can serve as an informative supervision for the training of the fast learner itself. However, replaying the self-predicted pseudo labels on the fast learner fails to prevent forgetting, as indicated by the drop from -5.48% to -4.83% in F. It is possible that the pseudo labels generated by the fast learner only bias towards the classes which have already been learnt very well and fail to reinforce the fast learner to improve on the poorly-learned classes. Different from the fast learner, the slow learner integrates semantic information over time. The predicted pseudo labels carry more semantic information, which is useful for fast learner to capture more generic object representations during pseudo label replays. Again, this emphasizes that the reciprocal replay from the slow learner to the fast learner is critical for memory reinstatement, which has been missing in the computational modeling literature of CLS.

## 6 Conclusion

To imitate what humans see and learn in the real world, we introduced a more realistic and challenging problem on label-efficient online continual object detection in video streams. Addressing this problem would greatly benefit real-world applications by reducing model retraining time and data annotation costs. Inspired by the complementary learning systems (CLS) in human brains, we proposed Efficient-CLS. Just like humans, it is capable of learning to detect objects continuously from both fully and sparsely annotated video streams, while retaining previously learnt knowledge. We rigorously evaluated Efficient-CLS and competitive baselines on two challenging real-world video stream datasets. We verified the effectiveness of our method in reducing annotation costs and avoiding catastrophic forgetting. Although our Efficient-CLS only capitalizes on 25% annotations, it beats all comparative models requiring fully supervised training on all video streams. Despite the promising results of our Efficient-CLS, we still observed a large performance gap between Efficient-CLS and the

object detection algorithms trained in the offline setting, highlighting the challenges in our introduced LEOCOD problem.

## References

- [1] Rahaf Aljundi, Eugene Belilovsky, Tinne Tuytelaars, Laurent Charlin, Massimo Caccia, Min Lin, and Lucas Page-Caccia. Online continual learning with maximal interfered retrieval. *Advances in neural information processing systems*, 32, 2019.
- [2] Rahaf Aljundi, Min Lin, Baptiste Goujaud, and Yoshua Bengio. Gradient based sample selection for online continual learning. *Advances in neural information processing systems*, 32, 2019.
- [3] Elahe Arani, Fahad Sarfraz, and Bahram Zonooz. Learning fast, learning slow: A general continual learning method based on complementary learning system. *arXiv preprint arXiv:2201.12604*, 2022.
- [4] Lucas Caccia, Rahaf Aljundi, Nader Asadi, Tinne Tuytelaars, Joelle Pineau, and Eugene Belilovsky. New insights on reducing abrupt representation change in online continual learning. *arXiv preprint arXiv:2203.03798*, 2022.
- [5] Hung-Jen Chen, An-Chieh Cheng, Da-Cheng Juan, Wei Wei, and Min Sun. Mitigating forgetting in online continual learning via instance-aware parameterization. *Advances in Neural Information Processing Systems*, 33:17466–17477, 2020.
- [6] Serena M Dudek and Mark F Bear. Bidirectional long-term modification of synaptic effectiveness in the adult and immature hippocampus. *Journal of Neuroscience*, 13(7):2910–2918, 1993.
- [7] Mark Everingham, SM Eslami, Luc Van Gool, Christopher KI Williams, John Winn, and Andrew Zisserman. The pascal visual object classes challenge: A retrospective. *International journal of computer vision*, 111(1):98–136, 2015.
- [8] Enrico Fini, Stéphane Lathuiliere, Enver Sangineto, Moin Nabi, and Elisa Ricci. Online continual learning under extreme memory constraints. In *European Conference on Computer Vision*, pages 720–735. Springer, 2020.
- [9] Kristen Grauman, Andrew Westbury, Eugene Byrne, Zachary Chavis, Antonino Furnari, Rohit Girdhar, Jackson Hamburger, Hao Jiang, Miao Liu, Xingyu Liu, et al. Ego4d: Around the world in 3,000 hours of egocentric video. *arXiv preprint arXiv:2110.07058*, 3, 2021.
- [10] Kaiming He, Xiangyu Zhang, Shaoqing Ren, and Jian Sun. Deep residual learning for image recognition. In *Proceedings of the IEEE conference on computer vision and pattern recognition*, pages 770–778, 2016.
- [11] Jisoo Jeong, Seungeui Lee, Jeesoo Kim, and Nojun Kwak. Consistency-based semi-supervised learning for object detection. *Advances in neural information processing systems*, 32, 2019.
- [12] Daoyun Ji and Matthew A Wilson. Coordinated memory replay in the visual cortex and hippocampus during sleep. *Nature neuroscience*, 10(1):100–107, 2007.
- [13] Nitin Kamra, Umang Gupta, and Yan Liu. Deep generative dual memory network for continual learning. *arXiv preprint arXiv:1710.10368*, 2017.
- [14] James Kirkpatrick, Razvan Pascanu, Neil Rabinowitz, Joel Veness, Guillaume Desjardins, Andrei A Rusu, Kieran Milan, John Quan, Tiago Ramalho, Agnieszka Grabska-Barwinska, et al. Overcoming catastrophic forgetting in neural networks. *Proceedings of the national academy of sciences*, 114(13):3521–3526, 2017.
- [15] Dharshan Kumaran, Demis Hassabis, and James L McClelland. What learning systems do intelligent agents need? complementary learning systems theory updated. *Trends in cognitive sciences*, 20(7):512–534, 2016.
- [16] Brenden M Lake, Tomer D Ullman, Joshua B Tenenbaum, and Samuel J Gershman. Building machines that learn and think like people. *Behavioral and brain sciences*, 40, 2017.
- [17] Yen-Cheng Liu, Chih-Yao Ma, Zijian He, Chia-Wen Kuo, Kan Chen, Peizhao Zhang, Bichen Wu, Zsolt Kira, and Peter Vajda. Unbiased teacher for semi-supervised object detection. *arXiv preprint arXiv:2102.09480*, 2021.
- [18] Juan-Manuel Perez-Rua, Xiatian Zhu, Timothy M Hospedales, and Tao Xiang. Incremental few-shot object detection. In *Proceedings of the IEEE/CVF Conference on Computer Vision and Pattern Recognition*, pages 13846–13855, 2020.
- [19] Quang Pham, Chenghao Liu, and Steven Hoi. Dualnet: Continual learning, fast and slow. *Advances in Neural Information Processing Systems*, 34, 2021.
- [20] Quang Pham, Chenghao Liu, Doyen Sahoo, and HOI Steven. Contextual transformation networks for online continual learning. In *International Conference on Learning Representations*, 2020.
- [21] Sylvestre-Alvise Rebuffi, Alexander Kolesnikov, Georg Sperl, and Christoph H Lampert. icarl: Incremental classifier and representation learning. In *Proceedings of the IEEE conference on Computer Vision and Pattern Recognition*, pages 2001–2010, 2017.

- [22] Shaoqing Ren, Kaiming He, Ross Girshick, and Jian Sun. Faster r-cnn: Towards real-time object detection with region proposal networks. *Advances in neural information processing systems*, 28, 2015.
- [23] Mohammad Rostami, Soheil Kolouri, and Praveen K Pilly. Complementary learning for overcoming catastrophic forgetting using experience replay. *arXiv preprint arXiv:1903.04566*, 2019.
- [24] Dongsub Shim, Zheda Mai, Jihwan Jeong, Scott Sanner, Hyunwoo Kim, and Jongseong Jang. Online class-incremental continual learning with adversarial shapley value. In *Proceedings of the AAAI Conference on Artificial Intelligence*, volume 35, pages 9630–9638, 2021.
- [25] Kihyuk Sohn, Zizhao Zhang, Chun-Liang Li, Han Zhang, Chen-Yu Lee, and Tomas Pfister. A simple semi-supervised learning framework for object detection. *arXiv preprint arXiv:2005.04757*, 2020.
- [26] Yihe Tang, Weifeng Chen, Yijun Luo, and Yuting Zhang. Humble teachers teach better students for semi-supervised object detection. In *Proceedings of the IEEE/CVF Conference on Computer Vision and Pattern Recognition*, pages 3132–3141, 2021.
- [27] Jianren Wang, Xin Wang, Yue Shang-Guan, and Abhinav Gupta. Wanderlust: Online continual object detection in the real world. In *Proceedings of the IEEE/CVF International Conference on Computer Vision*, pages 10829–10838, 2021.
- [28] Yaqing Wang, Quanming Yao, James T Kwok, and Lionel M Ni. Generalizing from a few examples: A survey on few-shot learning. *ACM computing surveys (csur)*, 53(3):1–34, 2020.
- [29] Jaehong Yoon, Divyam Madaan, Eunho Yang, and Sung Ju Hwang. Online coreset selection for rehearsal-based continual learning. *arXiv preprint arXiv:2106.01085*, 2021.
- [30] Mengmi Zhang, Rohil Badkundri, Morgan B Talbot, Rushikesh Zawar, and Gabriel Kreiman. Hypothesis-driven stream learning with augmented memory. *arXiv preprint arXiv:2104.02206*, 2021.
- [31] Qiang Zhou, Chaohui Yu, Zhibin Wang, Qi Qian, and Hao Li. Instant-teaching: An end-to-end semi-supervised object detection framework. In *Proceedings of the IEEE/CVF Conference on Computer Vision and Pattern Recognition*, pages 4081–4090, 2021.
- [32] Barret Zoph, Ekin D Cubuk, Golnaz Ghiasi, Tsung-Yi Lin, Jonathon Shlens, and Quoc V Le. Learning data augmentation strategies for object detection. In *European conference on computer vision*, pages 566–583. Springer, 2020.

## A Appendix

### A.1 Additional Experimental Details

#### A.1.1 Training

For a fair comparison, we follow the prior work [27] to use Faster-RCNN [22] with ResNet-50 backbone [10] as our object detection network, which is initialized by the weights pre-trained on PASCAL VOC [7]. We use Adam optimizer with a learning rate 0.0001, and the batch size is set to 16 frames. Same as [27], we maintain a replay buffer with 5 samples per class. At each time step  $t$ , we first randomly retrieve 16 video frames from the replay buffer for joint training. We use confidence thresh  $\tau = 0.7$  to generate pseudo-labels for unlabeled frames. Data augmentation, including random image crops, rotations, and horizontal flip, is applied on these pseudo-labeled frames. We introduce  $\lambda_{pseudo} = 1.0$  as a hyper-parameter to balance the contribution of two losses  $\mathcal{L}_{sup}$  and  $\mathcal{L}_{pseudo}$ . After updating the weights of the fast learner via backpropagation of the incurred losses, we update the slow learner by taking the EMA of the fast learner’s weights with an EMA rate  $\alpha = 0.99$ . Finally, the replay buffer is updated with the labeled frame at current time step  $t$ . Each model is trained by a single pass over the entire video stream. The training is carried out on 2 NVIDIA RTX 3090 GPUs.

#### A.1.2 Evaluation Metrics

Following [27], we evaluate all the methods with three standard metrics: continual average precision (CAP), final average precision (FAP) and forgetfulness (F). We adopt AP50, *i.e.*, the average precision (AP) at IoU = 0.5, as the measurement of AP.

**CAP** shows the average performance of a continual learning algorithm over the time span of the entire video stream. As shown in Figure 1, the model is evaluated on the test set every 100 time steps. At  $i^{th}$  evaluation step, the reported  $CAP_{t_i}$  is defined as

$$CAP_{t_i} = \frac{1}{C} \sum_{c=0}^C CAP_{t_i}^c, \quad (S1)$$

where  $CAP_{t_i}^c$  is the average precision (AP) of the class  $c$  on the test set. CAP is then defined as the average values over all the evaluation steps:

$$CAP = \frac{1}{N} \sum_{i=0}^N CAP_{t_i} = \frac{1}{NC} \sum_{i=0}^N \sum_{c=0}^C CAP_{t_i}^c, \quad (S2)$$

where  $N$  is the total evaluation steps.

**FAP** is the final performance of a model after seeing the entire video. That is,  $FAP = CAP_{t_N}$ , where  $t_N$  denotes the last evaluation step.

**F** estimates the forgetfulness of the model due to the sequential training. It takes into account the time interval between the presence of an object category and its subsequent presence. For a class  $c$ , we sort the  $CAP_{t_i}^c$  according to the time interval  $k$  between evaluation time  $t_i$  and the last time  $t_i - k$  the model is trained on  $c$ . After  $CAP_{t_i}^c$  is sorted, all  $CAP_{t_i}^c (i = 0, \dots, T)$  are divided into  $K$  bins  $B_{kmin}, \dots, B_{kmax}$  according to the time interval  $k$ . The average CAP ( $aCAP_k$ ) of each bin  $B_k$  is defined as the model’s performance for detecting class  $c$  after the model has not been trained on  $c$  for  $k$  time steps. The forgetfulness (F) of the class  $c$  is defined as the weighted sum of the performance decrease at each time:

$$F^c = \sum_{k=kmin}^{kmax} \frac{k - kmin}{\sum_{k=kmin}^{kmax} k - kmin} \times (aCAP_{kmin} - aCAP_k). \quad (S3)$$

The overall forgetfulness is then defined as:

$$F = \frac{1}{C} \sum_{c=0}^C F^c \quad (S4)$$

### A.1.3 Datasets

**OAK.** We follow [27] in the ordering of training and testing data splits, *i.e.*, one frame every 16 consecutive video frames is held out to construct a test set and the remaining frames are used for training. However, as the original test set curated by [27] is not publicly available, we re-split the training and testing data using the video streams from the original training set. The model trained and evaluated on our dataset shows comparable results with the original one.

**EgoObjects.** The original data can be downloaded from this website<sup>4</sup>. This dataset consists of 6076 videos taken in 1110 realistic indoor environments (around 6 videos per environment). The videos in each environment contain the same objects but feature a great variety of lighting conditions, scale, camera motion, and background complexity. We first downsample the original videos by 2 frames to make the length of the entire video stream comparable with OAK dataset. We shuffle the ordering of 6076 videos (not the video frames from the same video) from different environments to make it more realistic as the previously seen environments are allowed to be revisited in real-world. We concatenate the videos as one long video stream, and use the same ordering as OAK to construct the train and test data splits.

## A.2 Additional Ablation Study

In addition to the ablation studies provided in the main paper, we further study the effectiveness of each component in our proposed Efficient-CLS in the following sections.

### A.2.1 Effect of EMA and Pseudo-labeling

In the main text, we studied the effect of EMA and pseudo-labeling at 12.5% annotation costs (Section 5.3). Here we performed the same experiments at annotation costs 6.25% (Table S1), 25% (Table S2), and 50% (Table S3). We found that, by integrating the EMA and pseudo-labeling, our Efficient-CLS (4th row) improves the state-of-the-art model (1st row) and other ablated models (2nd row and 3rd row) by a significant margin. Please refer to Section 5.3 for more analysis.

Table S1: Effectiveness of Exponential Moving Average (EMA) and Pseudo-labeling on OAK dataset at annotation cost 6.25%. The best results are **bold-faced**.

EMA	Pseudo-labeling	FAP ( $\uparrow$ )	CAP ( $\uparrow$ )	F ( $\downarrow$ )
$\times$	$\times$	23.04	17.75	-3.31
$\checkmark$	$\times$	27.84	20.03	-3.96
$\times$	$\checkmark$	26.39	19.50	-1.99
$\checkmark$	$\checkmark$	<b>29.72</b>	<b>20.31</b>	<b>-5.36</b>

Table S2: Effectiveness of Exponential Moving Average (EMA) and Pseudo-labeling on OAK dataset at annotation cost 25%. The best results are **bold-faced**.

EMA	Pseudo-labeling	FAP ( $\uparrow$ )	CAP ( $\uparrow$ )	F ( $\downarrow$ )
$\times$	$\times$	33.70	24.57	-4.30
$\checkmark$	$\times$	34.79	25.62	-4.35
$\times$	$\checkmark$	34.95	25.65	-3.65
$\checkmark$	$\checkmark$	<b>38.36</b>	<b>26.64</b>	<b>-8.20</b>

Table S3: Effectiveness of Exponential Moving Average (EMA) and Pseudo-labeling on OAK dataset at annotation cost 50%. The best results are **bold-faced**.

EMA	Pseudo-labeling	FAP ( $\uparrow$ )	CAP ( $\uparrow$ )	F ( $\downarrow$ )
$\times$	$\times$	34.68	25.78	-4.15
$\checkmark$	$\times$	35.74	25.77	-4.82
$\times$	$\checkmark$	35.61	25.56	-3.76
$\checkmark$	$\checkmark$	<b>38.61</b>	<b>26.90</b>	<b>-7.29</b>

<sup>4</sup><https://sites.google.com/view/clvision2022/challenge>



### A.2.2 Effect of EMA Rates

As mentioned in Section 5.3, we varied  $\alpha$  from 0.5 and 0.999 and presented their performance in Table S4. We observed that the choice of  $\alpha$  is relatively insensitive to the performance. For example, Efficient-CLS with  $\alpha = 0.9$  leads to a performance increase of less than 1% in FAP and CAP and 1.12% in F, compared with the case of  $\alpha = 0.5$ . However, we did observe a huge performance drop when  $\alpha$  is very close to 1.0, where there is almost no synaptic weight transfer between slow and fast learner.

Table S4: Ablation study of varying EMA rates  $\alpha$  on OAK dataset in fully supervised protocol.

$\alpha$	0.5	0.9	0.95	0.99	0.995	0.999
FAP ( $\uparrow$ )	36.93	37.57	38.25	40.24	40.59	33.02
CAP ( $\uparrow$ )	26.70	28.35	28.61	28.18	27.11	15.15
F ( $\downarrow$ )	-6.66	-5.54	-6.20	-8.10	-9.70	-5.72

### A.2.3 Effect of Pseudo-labeling Threshold

As mentioned in Section 3.2, we apply confidence thresholding to remove predicted bounding boxes that have low confidence scores. To show the effectiveness of thresholding, we varied the confidence threshold  $\tau$  from 0.1 to 0.9 (see Table S5). We observed that the model using a high threshold (*e.g.*, 0.7) yields satisfactory results, as it produces more reliable pseudo-labels with high confidence. On the other hand, using a low threshold can result in lower performance since the model generates too many bounding boxes, which are likely to be false positives.

Table S5: Ablation study of varying confidence threshold  $\tau$  at annotation cost 12.5%.

$\tau$	0.1	0.3	0.5	0.6	0.7	0.8	0.9
FAP ( $\uparrow$ )	30.33	31.16	32.17	32.54	33.92	32.81	32.07
CAP ( $\uparrow$ )	21.45	21.67	22.38	22.51	23.04	22.69	22.70
F ( $\downarrow$ )	-7.11	-7.29	-6.88	-6.98	-7.71	-6.60	-6.94

### A.2.4 Effect of RPN Loss in Pseudo Training

In Section 3.2, we mentioned that pseudo losses are only applied at the ROI module but not at the RPN module. As shown in Table S6, the model with and without RPN loss in training pseudo-labeled frames show similar performance. We assumed that the RPN module is less likely to suffer catastrophic forgetting since its primary function is to produce general proposals that are class agnostic. As a result, we removed the RPN loss during pseudo training, which also reduces the overall computational cost.

Table S6: Performance of our Efficient-CLS with and without RPN loss in pseudo training on OAK dataset at annotation cost 12.5%. The best results are bold-faced.

RPN Loss	FAP ( $\uparrow$ )	CAP ( $\uparrow$ )	F ( $\downarrow$ )
$\times$	<b>33.92</b>	<b>23.04</b>	<b>-7.71</b>
$\checkmark$	33.64	22.68	-7.62

### A.2.5 Effect of Pseudo Loss Weights

As mentioned in Section 3.2,  $\lambda_{pseudo}$  is a hyperparameter balancing the importance of supervised loss ( $\mathcal{L}_{sup}$ ) and pseudo loss ( $\mathcal{L}_{pseudo}$ ). To examine the effect of  $\lambda_{pseudo}$ , we varied the  $\lambda_{pseudo}$  from 0.5 to 4.0 at annotation cost 12.5% on OAK dataset. As shown in Table S7, the model performs the best with  $\lambda_{pseudo} = 1.0$  and shows moderate performance drop for other values of  $\lambda_{pseudo}$  (0.5, 1.5, and 2.0). However, when  $\lambda_{pseudo}$  is set to 4.0, the model performance deteriorates.

### A.2.6 Effect of Data Augmentation in Pseudo Training

As mentioned in Section 3.2, we use data augmentation techniques when training the pseudo-labeled frames. Here we ablated our Efficient-CLS by removing data augmentation in pseudo training. From

Table S7: **Ablation study of varying pseudo loss weights  $\lambda_{pseudo}$  at annotation cost 12.5%.**

$\lambda_{pseudo}$	0.5	1.0	1.5	2.0	4.0
FAP ( $\uparrow$ )	33.19	33.92	33.01	32.67	30.08
CAP ( $\uparrow$ )	22.92	23.04	22.52	22.02	20.17
F ( $\downarrow$ )	-6.55	-7.71	-7.71	-7.86	-7.50

Table S8 at annotation cost 12.5%, we observed that removing data augmentation in pseudo training leads to a performance drop of 3.60% in FAP, 1.96% in CAP and 1.21% in F on OAK dataset. This indicates that using data augmentation on pseudo-labeled frames can enforce the model to learn invariant object representations from these video frames.

Table S8: **Effectiveness of Data Augmentation in Pseudo Training on OAK dataset at annotation cost 12.5%.** The best results are **bold-faced**.

Data Augmentation	FAP ( $\uparrow$ )	CAP ( $\uparrow$ )	F ( $\downarrow$ )
$\times$	30.32	21.08	-6.50
$\checkmark$	<b>33.92</b>	<b>23.04</b>	<b>-7.71</b>

### A.3 Analysis of Unlabeled Frames Selection

See caption in Table S9.

Table S9: **Performance of our Efficient-CLS on OAK dataset in sparse annotation protocol.** The table header denotes the percentage of frames that are labeled in the video stream. We conducted each experiment with 5 runs. Each run has a different random seed. The means and standard deviations in brackets are reported. We find that our Efficient-CLS shows reliable and robust performance against different selections of unlabeled frames in the video stream.

Annotation Cost (%)	50	25	12.5	6.25
FAP ( $\uparrow$ )	38.45 ( $\pm 0.68$ )	38.00 ( $\pm 1.17$ )	34.29 ( $\pm 0.76$ )	30.50 ( $\pm 1.07$ )
CAP ( $\uparrow$ )	26.85 ( $\pm 0.24$ )	26.38 ( $\pm 0.32$ )	23.47 ( $\pm 0.73$ )	20.60 ( $\pm 0.43$ )
F ( $\downarrow$ )	-8.01 ( $\pm 0.77$ )	-8.32 ( $\pm 0.98$ )	-7.30 ( $\pm 0.82$ )	-6.28 ( $\pm 0.69$ )

### A.4 Analysis of AP Changes over Time

See caption in Figure S1.

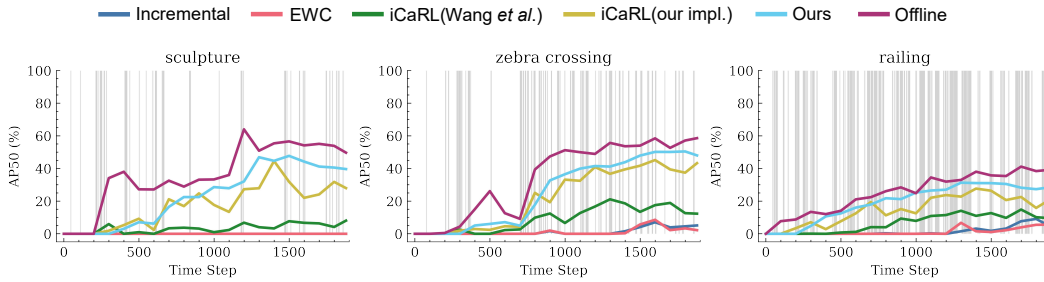


Figure S1: **The changes of  $CAP_{t_i}^c$  with sampled categories on OAK dataset in fully supervised protocol.** The x-axis denotes the time step across the entire video stream. The y-axis denotes the AP50 of the category at specific time step (*i.e.*,  $CAP_{t_i}^c$ ). The grey line indicates the existence of the category. Our method (light blue) consistently outperforms existing approaches with minimal forgetting even when categories appear infrequently (*e.g.*, sculpture) and exhibits the closest gap against the upper bound (Offline).

### A.5 Analysis of Inference Model

See caption in Figure S2.

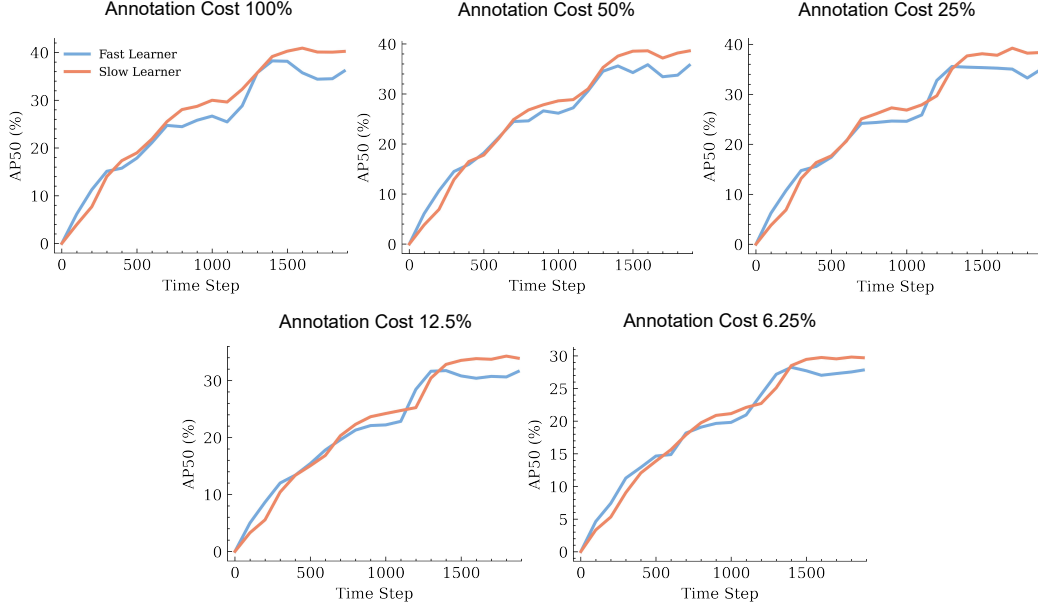


Figure S2: **The changes of  $CAP_{t_i}$  on OAK dataset at different annotation costs.** The x-axis denotes the time steps across the entire video stream. The y-axis denotes the AP50 at specific time step (*i.e.*,  $CAP_{t_i}$ ). This plot shows that the slow learner (orange) of our Efficient-CLS is better at preventing forgetting than the fast learner (blue), hence we used the slow learner at inference stage (Section 5.3).

#### A.6 Visualization of Pseudo-labeling

See caption in Figure S3.



Figure S3: **Visualization of example pseudo-labels predicted by our Efficient-CLS and the Naive Pseudo-labeling.** The white box with dash line denotes the ground truth label. The box with solid line denotes the pseudo-labels (the ones in green are correct while the red are wrong labels). The **Naive Pseudo-labeling** only has one learner and uses the pseudo-labels generated by itself for training. This plot shows that the pseudo-labels generated by our **Efficient-CLS** (2nd column) capture more ground truth objects and contain fewer false positive instances than the **Naive Pseudo-labeling** model (1st column).